3D Imaging Reveals Resilience: Storm Impact on Coral Reef Structural Complexity

Matan Yuval[1,2,3] | Naama Pearl[1] | Dan Tchernov[2] | Stephane Martinez[2] | Yossi Loya[4] | Avi Bar-Massada[5] | Tali Treibitz[1]

[1]Marine Imaging Lab, Hatter Department of Marine Technologies, University of Haifa, Haifa 3498838, Israel

[2]Department of Marine Biology, University of Haifa, Haifa 3498838, Israel

[3]The Interuniversity Institute for Marine Sciences of Eilat, Eilat 8810302, Israel

[4]School of Zoology, Tel-Aviv University, Tel Aviv 6997801, Israel

[5]Department of Biology and Environment, University of Haifa at Oranim, Kiryat Tivon 36006, Israel

Correspondence
Matan Yuval, The Interuniversity Institute for Marine Sciences of Eilat, Eilat 8810302, Israel
Email: mtnyvl@gmail.com

Abstract

Extreme weather events are increasing in frequency and magnitude. Consequently, it is important to understand their effects and remediation. Resilience reflects the ability of an ecosystem to absorb change, which is important for understanding dynamics and predicting phase shifts. We describe the impact of a powerful storm on coral reef structural complexity, serving as a case study on coral reef resilience.

We used novel computational tools and detailed 3D reconstructions captured at three time-points over three years. Our data-set ***Reefs4D*** of 21 co-registered image-based models enabled us to calculate the differences at seven sites over time and is released with the paper. We employed six geometrical metrics, two of which are new algorithms for calculating fractal-dimension of reefs in full 3D. We conducted a multivariate analysis to reveal which sites were affected the most and their relative recovery. We also explored the changes in fractal dimension per size category using our cube-counting algorithm.

Three metrics showed a significant difference between time-points, i.e., decline and subsequent recovery in structural complexity. The multivariate analysis and the results per size category showed a similar trend.

Coral reef resilience has been the subject of seminal studies in ecology. We add important information to the discussion by focusing on 3D structure through image-based modeling. The full picture presents a new view on resilience, suggesting that the reef has not gone through a phase-shift and is returning to its prior state w.r.t. structural complexity. Our novel analysis framework is widely transferable and useful for research, monitoring, and management.

Keywords: Coral-reefs, Fractal dimension, 3D change detection, Resilience, Extreme weather events.

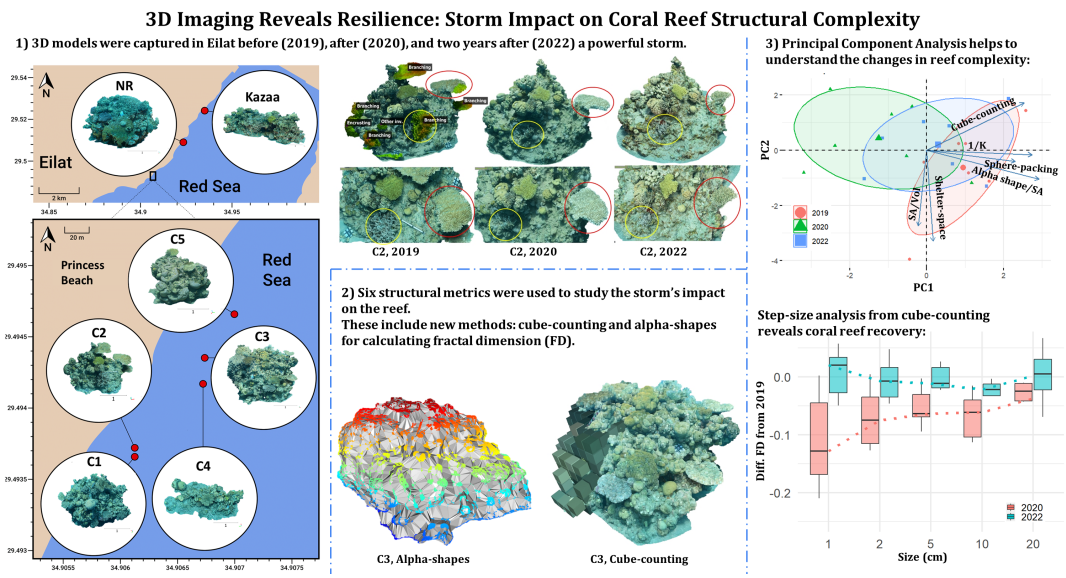

Graphical Abstract

1 | INTRODUCTION

Coral reefs are some of the most important ecosystems on the planet. However, they are undergoing major negative changes due to human activities (Hughes et al. 2003; Hoegh-Guldberg and Bruno 2010; Hughes et al. 2017). 3D photogrammetry is increasingly being used to monitor coral reefs, but so far it is not exploited to its full potential, i.e., there is still significant underlying information in these models that currently is not used.

Here we aim to explore resilience via automated analysis of 3D coral reef models. Resilience is defined as the amount of disturbance that an ecosystem can absorb without changing self-organized processes and structures (Holling 1973; Gunderson 2000). This raises the question: what are the steady states in a transient system, e.g., coral reefs (Standish et al. 2014)? Phase shifts in coral reefs have been most commonly described as a transition to algae-dominated reefs (Hughes 1994; Crisp et al. 2022). Although many studies have focused on coral reef resilience (Dudgeon et al. 2010; Nyström and Folke 2001), much remains to be learned on the response of reefs to extreme weather events and major storms (Roff and Mumby 2012). Storms can have mixed effects on reefs such as a decrease in live cover leading to increased diversity (Rogers 1993). Hurricanes have been shown to reduce the cover of dominant fragile forms and to generate space on the reef (Porter et al. 1981). Cyclones can even contribute to the maintenance of diversity by preventing monopolization and increasing habitat fragmentation (Harmelin-Vivien 1994). However, some of the most negative effects of storms are changes in the topographic structure of the reef, which can lead to an ecosystem collapse through various cascaded pathways.

Structural complexity denotes the amount of structural features, their sizes, and distribution. In coral reefs, biodiversity and structural complexity are clearly linked (Graham and Nash 2013; Ferrari et al. 2016; Alvarez-Filip et al. 2009). Therefore, although resilience was traditionally studied through metrics of community composition (species richness and diversity), here we demonstrate that structural complexity is a suitable proxy for reef-state in phase-shift studies. Moreover, community composition metrics are difficult to obtain from image-based surveys because they require laborious annotations (classifying pixels in an image). On the contrary, structural complexity metrics can be extracted automatically (without annotations), making them more feasible to employ over large scales.

We examine reef structural complexity before and after an extreme weather event- a powerful storm, across three years. Resilience corresponds with the amount of disturbance that a system can absorb before shifting to a different state (Connell and Sousa 1983).

Photogrammetry- three-dimensional (3D) imaging, has emerged as an effective and popular method for benthic surveys (Ferrari et al. 2022). Photogrammetry has been used to measure the rugosity (Friedman et al. 2012), habitat structural complexity (Ferrari et al. 2016), fractal dimension (FD), vector dispersion (Young et al. 2017; Torres-Pulliza et al. 2020; Aston et al. 2022), shelter capacity (Urbina-Barreto et al. 2021; Hylkema et al. 2020) and even to study the impact of storms (Pascoe et al. 2021). Nevertheless, much remains to be learned on the best way to analyze 3D models at the whole reef scale over time and in full 3D as structural complexity can be expressed through various measures that are not always in agreement.

Fractals are self-similar structures that have gained traction across science and industry since the seminal work of Mandelbrot (Mandelbrot 1967), where the classic example of fractal dimension deals with measuring the length of the coastline of England. The length increases when increasing the resolution of the measuring tool and vice-versa. Although natural systems are not truly self-similar nor fractal, the concept of fractal dimension (FD) is useful in a broad range of applications from computer graphics to economy and ecology (Barnsley 2014; Sugihara and May 1990). FD can be examined in size categories by calculating the slope of each two measurements (Fig. 5), methods 2.3.1 (Walsh and Watterson 1993. This provides information not only on niche availability for various taxa but also on the size-frequency distribution of structural features. Therefore, FD is a powerful descriptor of structural complexity (Halley

et al. 2004) and important for the scope of coral reef ecology where many of the interactions are size-dependent (e.g., fish use corals for shelter) (Rogers et al. 2014).

Fractal geometry has been employed to study coral reefs *in situ* (Knudby and LeDrew 2007), and more recently has been also employed on Digital Elevation Models (DEMs, where each pixel is a height value) (McCarthy et al. 2022), as well as using surface smoothing (Young et al. 2017), and volume-packing (Fukunaga and Burns 2020; Reichert et al. 2017) as means to assess FD.

Space-filling is a property of objects that exist between euclidean dimensions (e.g., lines that make surfaces, surfaces that make volumes). This is a prevalent characteristic of hierarchical networks- circulatory systems to cities and ecosystems. Measuring an object at several resolutions or scales enables estimating the degree of complication and the amount of space-filling, as complex shapes tend to reveal more details at higher resolutions. However, fractal dimension remains challenging to measure in many ecological systems. Measuring it from 2.5D representations (Young et al. 2017) fails to account for overhangs which are a key feature of reefs and provide habitat for many taxa.

The Minkowski-Bouligand (box/cube counting) dimension is one of the most common methods for measuring FD. Although there are many implementations of box-counting in 2D, and even on voxel-clouds (Fukunaga and Burns 2020) and single coral colonies (George et al. 2021), to the best of our knowledge cube counting has never been implemented before on wide-scale 3D models of coral reefs. To bridge this gap, we developed two methods for calculating FD in 3D, a method for cube-counting on a 3D mesh, and a surface-based method with alpha shapes (a surface smoothing filter) (Edelsbrunner et al. 1983) and surface-area (SA) ratios (alpha-shapes/SA). Measuring SA at different levels of surface-smoothing enables to calculate the dimension as a flat surface will not decrease in surface area when applying a smoothing filter.

We also used the software released by (Reichert et al. 2017) for sphere-influence, and three other metrics: surface area over volume (SA/Vol), shelter-space (a normalized version of (Hylkema et al. 2020), and vector dispersion (1/k) following (Young et al. 2017). We examined each variable separately and conducted a multivariate analysis.

To summarize, we employed and analyzed six 3D geometrical metrics to uncover the changes in structural complexity of seven reef sites in Eilat, Northern Red-Sea, over a three-year (2019-2022) period. We release the ***Reefs4D*** data-set, comprising of 21 3D models at three time-points: before, immediately after, and two years after a powerful storm. We also release our code for two new fractal dimension methods that operate in full 3D and can help in research and monitoring activities. We present a novel analysis framework and an original case study of the effects of an extreme weather event on coral reefs using 3D geometric methods on the ecosystem scale, revealing a trend of reef resilience in a two-year time-frame post-disturbance.

2 | METHODS

2.1 | 3D imaging

Our workflow for 3D imaging is described in (Yuval et al. 2021). We use a DSLR camera to take overlapping images of the reef knolls from all angles of view and several distances. We used Agisoft Metashape[1] to process the 3D models by aligning the photos and building mesh from depth-maps.

[1]AgiSoft Metashape Professional (Version 1.5) (Software) Agisoft LLC, St. Petersburg, Russia, 2016.

2.2 | Data-set

Our data-set contains 21 models from seven shallow reef knolls at three distinct beaches that represent a different extent of damage following a natural disturbance (Fig. 2A). The models were captured during Aug-Sept 2019, June 2020, and July 2022. The storm struck Eilat in March 2020. The results are summarised in table 1.

2.3 | Structural complexity assessment

2.3.1 | Fractal dimension (FD) methods

We used three FD methods that differ in approach. These three methods enable estimating the amount of space-filling of surfaces by measuring a metric at several resolutions or scales. cube counting is an extrinsic approach that operates on a 3D grid while alpha shapes/SA is intrinsic and operates on the mesh surface. Sphere influence is an intrinsic variant of the Minkowski-Bouligand dimension.

| Cube counting for fractal dimension

One way to determine the fractal dimension of an object is the Minkowski-Bouligand or cube-counting dimension, which is given by the formula:

$$FD = \lim_{\epsilon \to 0} \frac{\log N(\epsilon)}{\log(1/(\epsilon))} \quad , \tag{1}$$

where ϵ is the size of the measuring element and N(ϵ) is the number of measuring elements required to cover the object. In 3D, the element is a cube, (ϵ) is the length of the cube, and N(ϵ) is the number of cubes required to cover the 3D object. This method calculates N(ϵ) for several lengths of ϵ and evaluates the fractal dimension as the slope of the fitted line between log(N(ϵ)) and log(1/ϵ).

Our implementation takes an input 3D mesh and bounds it with a minimal bounding cube. The cube is then divided into 8 equal cubes (each dimension is halved). In each iteration, cubes that contain a part of the mesh are counted, and only these cubes are then divided in the next iteration (Fig. 1A).

| Cube counting by step-size

Determining the FD per box size is done by measuring the slope between two points in the cube counting results (Walsh and Watterson 1993).

$$\mathrm{FD}_{\text{Size cateogry}(i)} = \frac{Y_{i+1} - Y_i}{X_{i+1} - X_i} \quad , \tag{2}$$

where Y is log(N(ϵ)) and X is log(1/ϵ) (from Eq. 1). The size category is determined by the size value (ϵ) of the smaller box size. Temporal differences are calculated by subtracting the FD values in corresponding size categories and models. We used the models from 2019 as a reference. Positive values indicate increasing complexity, and vice versa.

Alpha-shapes and surface-area

Alpha shapes are a generalization of the convex hull that depends on a size parameter- alpha, to construct a convex shape from a set of points (Edelsbrunner et al. 1983). By incrementing alpha different levels of detail on the set of points can be achieved, i.e., surface smoothing.

The alpha parameter is size-specific and can be used as a surface-smoothing threshold, enabling us to generate surface-smoothings at varying resolutions and different levels of detail. We calculated FD by incrementing the α value and measuring the surface area at each iteration (Fig. 1B). We used the following formula:

$$FD(\alpha) = 2 - \lim_{\alpha \to 0} \frac{\log(\text{SurfaceArea}(\alpha))}{\log(\alpha)} \quad , \tag{3}$$

where α is in a specified range (0.025, 0.05, 0.10, 0.2, 0.4, 0.6 m).

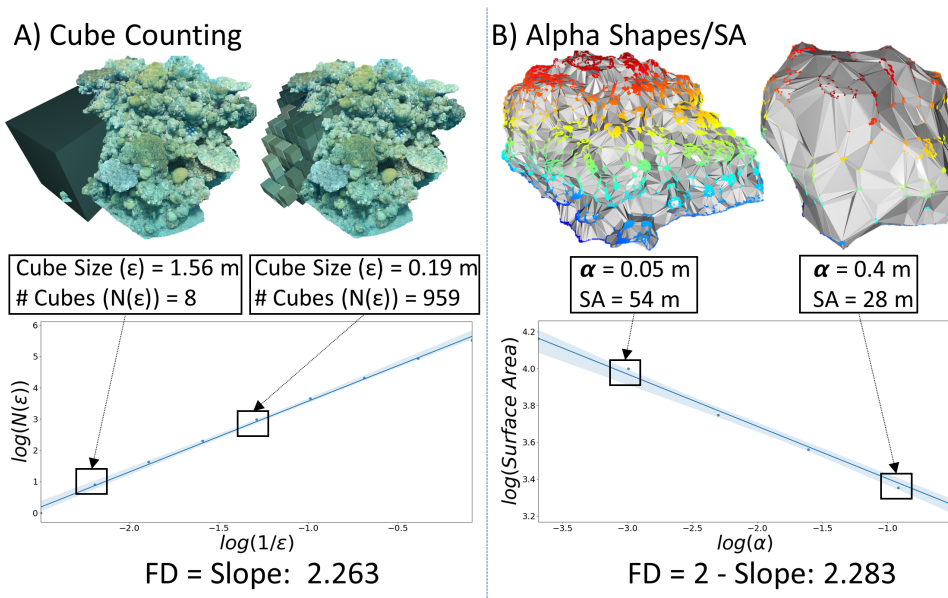

FIGURE 1 Methods for calculating FD from 3D on model C3. A) The cube counting method. The box lengths are ½ and 1/16 of the minimal bounding cube which are the second and fifth iterations in Cube-counting. Only the corner area of the model is used for visualization of cube-counting. B) The alpha-shapes/SA method shows the alpha shapes at 0.05 and 0.4 m. Surface area decreases with increase in alpha.

Sphere influence volume for fractal dimension

This measure calculates the fractal dimension using a variant of the Minkowski–Bouligand method- the sphere influence method. It places spheres of increasing radius on the mesh vertices and counts the number of interactions between spheres on the mesh. The ratio between sphere size and its influence (i.e., the number of interacting/overlapping spheres) defines the fractal dimension. To calculate this measure we used the software and guidelines

provided by the authors in (Reichert et al. 2017). The main disadvantage of their software is that its designed for single coral colonies and it stops at an upper limit of 20 cm of sphere influence.

2.3.2 | Surface Area (SA) / Volume

Surface area and volume were calculated in Metashape. This metric gives an idea regarding the surface complexity of the reef.

2.3.3 | Shelter-space

The shelter-space metric quantifies the amount of volume available for motile reef organisms in the immediate vicinity of the reef. We use the convex hull function of the mesh, which crudely encapsulates the object. We calculate the convex hull of the mesh in the open-source software Meshlab (Cignoni et al. 2008). We divide the volume of the 3D mesh by the volume of the convex hull to obtain the shelter-space metric using the following formula:

$$\text{Shelter} - \text{space} = 1 - \frac{\text{Mesh volume}}{\text{Convex} - \text{Hull volume}} \tag{4}$$

This metric ranges from 0 to 1 where 0 is no shelter-space and higher values mean more shelter-space.

2.3.4 | Vector dispersion 1/K

This metric is an estimate of the variance of the normals of the mesh. The result ranges between 0-1 indicating increasing complexity with increasing values. We calculated the direction cosines (cosine of the angle between the normal and each of the axes) of each face in the mesh using a custom Python script following (Young et al. 2017):

$$R_1 = \sqrt{\sum_{i=1}^{n} \cos(\alpha_{x,i})^2 + \sum_{i=1}^{n} \cos(\alpha_{y,i})^2 + \sum_{i=1}^{n} \cos(\alpha_{z,i})^2} \ . \tag{5}$$

where x,y,z are the angles between the ith normal and the x,y,z axis, accordingly, and n is the number of faces in the mesh.

$$\text{Vector Dispersion } 1/\text{k} = \frac{\text{n} - \text{R}_1}{\text{n} - 1} \tag{6}$$

2.4 | Code and data availability

Code will be made available at: https://github.com/MatanYuval/ReefMetrics
Data will be made available at: https://zenodo.org/

3 | RESULTS

3.1 | Visual change

We followed seven shallow (depth ~ 5 m) reef knolls in the Red Sea, Gulf of Aqaba (Eilat, map in Fig. 2A) by constructing high-resolution 3D photographic models for each reef at three time-point over three years (examples in Fig. 2B).

To enable change-detection and community-level data extraction (coral colony counts) from the 3D models, we conducted 3D registration. By overlaying corresponding models (the same reef over time), the differences can be visualized and help to identify areas of change in the reef (e.g., Fig. 2C). Moreover, registration is important for comparing the results of cube-counting over time because it is a rotation variant method. However, registration of dynamic scenes in 3D over time is a challenging problem because it requires static anchor points which in natural environments are inherently dynamic. The storm caused such a pronounced damage to the reef that when comparing the models from 2020 to 2019 we were able to count the number of coral colonies removed by the storm using manual registration and a mesh-to-mesh distance visualization (CloudCompare 2022 (Fig. 2C)). We found that the majority of corals removed (broken) by the storm were those with branching morphologies (Fig. 2D) which was probably due to their life-history traits and fast-growing fragile forms.

Comparing the models from 2022 to 2019 to quantify coral growth was much more challenging. Primarily, the registration was more difficult due to added changes over time. Second, the signal (coral growth) is much more mild compared to that of a full colony removal.

Moreover, tracking corals over time in 3D is not straightforward. Our results show that while some corals grow others decay, and even the same coral colony can show reverse trends. The close-up views in Fig. 2C show several examples. In model C2 (Fig. 2C, top) the coral colony in yellow is recovering and the one in red is decaying. In model C3 (Fig. 2C, middle), the colony in yellow is static while the one in red is growing rapidly. In C1 (Fig. 2C, bottom) the colony in yellow is decaying.

3.2 | Individual metrics for structural complexity assessment

We used six geometrical metrics for structural complexity on all 3D reef models (Fig. 3A, Supp. table 1), four known ones: surface area over volume (SA/Vol), shelter-space, vector dispersion (1/k), sphere-packing, and two new ones that we devised: cube counting, alpha-shapes/SA.

Cube-counting and alpha shapes/SA values were in the expected ranges of 2-3 which indicate a shape that is between a surface and a volume. The results of sphere-packing are in the range of those shown by the authors of this method (Reichert et al. 2017) which are slightly lower than two. In Fig. 3A, the site Kazaa (KZ) seems to change the least while the sites in Princess beach (C1- C5) show a temporal distribution with the lowest values generally in 2020 and the highest values in 2019.

We used a one-sided paired samples Wilcoxon test $(n_{pairs} = 7)$ to compare the difference in each variable from the baseline in 2019 (Fig. 3B). We tested whether the differences between 2019 and 2020 were more negative (smaller values) than the differences between 2019 and 2022. The difference was significant for cube-counting, alpha-shapes/SA, and SA/Vol with P-values of 0.0078, 0.0111, and 0.0078. The results were not significant for sphere-packing, 1/K, and shelter-space (P-values were 0.9609, 0.05469, and 0.4687).

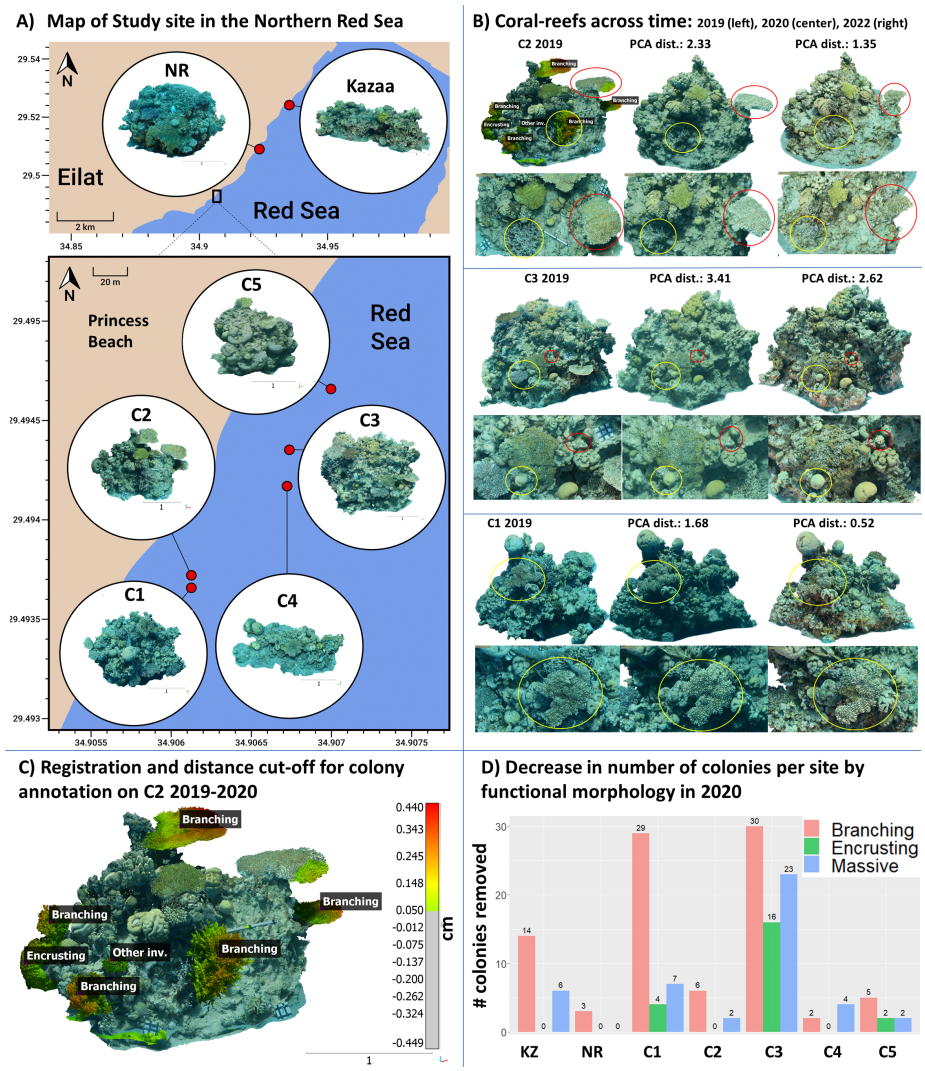

FIGURE 2 Coral reefs over time. A) A map of the ***Reefs4D*** data-set in the northern Gulf of Aqaba (GoA), Eilat. The top map shows the sites Kazaa (KZ, Oil Jetty), Nature reserve (NR), and Princess beach (C1-C5, close up on black rectangle). Each model is shown with a 1 m scale bar. B) Three reefs over time. The PCA distances for each model reflect the changes in structural complexity as shown in Fig. 4C. The circles mark corresponding areas in the models and the close-up views. In C2 (top) the coral colony in yellow is recovering and the one in red is decaying. In C3 (middle), the colony in yellow is static while the one in red is growing rapidly. In C1 (bottom) the colony in yellow is decaying. C) Registration and visualization of C2 in 2019 and 2020. The distance between models was calculated in *Cloudcompare* (CloudCompare 2022) software and a threshold (5 cm) were used to visualize and count the coral colonies that have been removed from the reef. D) A barplot of the colonies removed by the storm in each reef. Color indicates functional morphology. The majority of corals removed are branching.

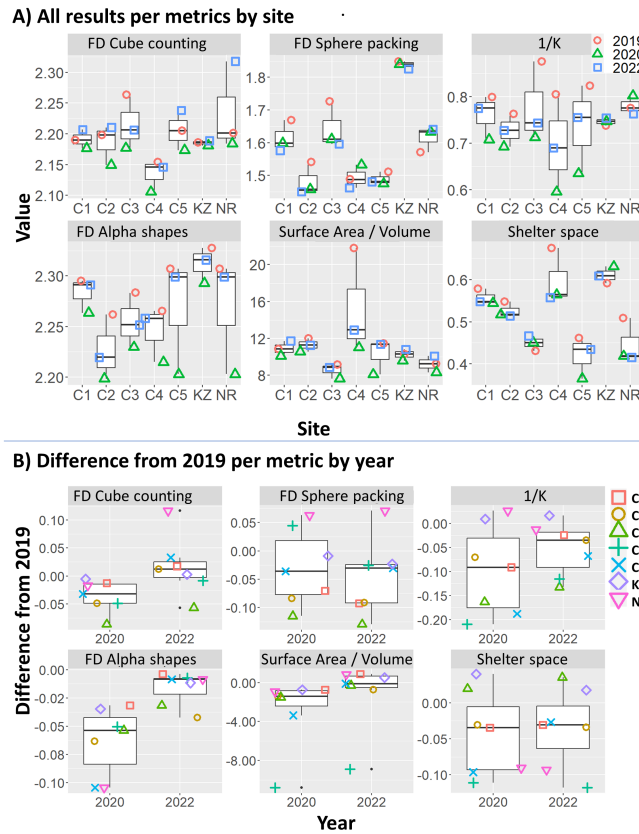

FIGURE 3 Metrics for structural complexity assessment. A) Results of all variables and all models. Color and shape indicate time. The medians are summarized in table 1. B) The difference in metric per year with the 2019 models as a reference. Color and shape indicate site. We used a paired samples Wilcoxon test ($n_{pairs} = 7$) with a one-sided alternative to test if the difference in each metric in 2020-2019 is smaller than the difference in 2020-2019. The difference was significant for cube-counting, alpha-shapes/SA, and SA/Vol with P-values of 0.0078, 0.0111, and 0.0078.

3.3 | Multivariate analysis

Testing each metric separately is very difficult because some metrics exhibit a recovery or even increasing values, while for the same site and year a different metric may show a decrease (e.g., cube counting and shelter-space on C3 2020, Fig. 3A). Combining the different variables helps to see how each site was affected and to reveal a complete picture of changes in the reef. To explore the relations between variables we calculated Pearson's correlation coefficient looking for highly correlated pairs (Fig. 4A). All variables had medium-to-low correlation (-0.48 to 0.61), demonstrating the importance of using more than one metric in describing the 3D structure of coral reefs.

We performed a Principal Component Analysis (PCA) to reduce the dimensionality of the data (Fig. 4B). The third principal component (PC3) explains less than 10% of the variance in the data and was excluded from the visualization. We found that PC1 correlates with 1/K, sphere-packing, and alpha-shapes. These are all intrinsic methods that operate on the mesh directly. In contrast, PC2 correlates with SA/Vol and shelter-space, both of which include the

mesh volume in their calculation. The ordination data points indicate a temporal trend of recovery mostly along PC1. Notably, the site Kazaa (KZ in Fig. 4A) remained clustered which matches our visual observation that it was affected the least and degraded the least.

We measured the distances of points on the first two PCA axes within site and across time, comparing them to the 2019 models as a baseline. The results of these measurements are presented in Fig. 4C. The red bars correspond with measurements taken right after the disturbance and depict a large difference from the baseline. The blue bars are shorter than the red bars in almost all of the sites, indicating that there is recovery in structural complexity.

Although this analysis is not directional (it is the Euclidean distance on two PCs, not decline or recovery), the shorter distances in 2019-2022 (red, Fig. 4C) indicate a positive trend of recovery and increasing structural complexity.

3.4 | Comparison of FD by size-category using cube counting

Note that the previous analysis is not indicative of size categories. Since reefs are composed of different structural features at multiple scales we wanted to further explore how the storm affected the reef in a size-dependent manner. We analyzed the FD per size category using the cube-counting method (Nash et al. 2013; Walsh and Watterson 1993). Measuring FD at several scales is a technique that was mostly used to plot the derivative of the curve (e.g., Fig. 1) looking for abrupt changes in slope that indicate a change in structural regime (Walsh and Watterson 1993), aka the Gibbs phenomena in the curve's limits (Backes and Bruno 2012).

To extract change per step size we calculated the slope between each pair of subsequent points in the cube counting results (e.g., Fig. 1A). We first noted the size in cm of each size category in the different models and then selected a threshold at step-size five (20 to 40 cm category). The sizes are determined as the average cube size per step. Because our calculation depends on the minimal bounding cube, larger variation occurs in the large-size categories, whereas the values converge in the small-size categories. For example, in the size category of 40 cm, we are dealing with the third iteration of cube counting where each box has more influence on FD, causing increased variation and sensitivity to rotation and registration.

In Fig. 5A we show the difference in FD per size category. We plotted the change per step-size at Princess beach (sites C1, C2, C3, C4, and C5) using 2019 as a reference (Fig. 5B). We chose to focus on these sites because they are located in the same beach and were the most exposed to the storm. The results show that there is less difference between the years 2019-2022 (red boxes) than between 2019-2020 (blue boxes), i.e., two years after the extreme weather event, indicating reef resilience: the reef is returning to its former cube-counting dimension.

4 | DISCUSSION

In coral reefs, structural complexity emerges from lower-level interactions between reef organisms (Jackson and Hughes 1985). To a large part, coral life histories and community-structure dictate the shape of the reef (Jones et al. 1994). The 3D structure is formed over large periods, retains memory, and encapsulates ecological information. Thus, it can be useful as a descriptor of ecosystem stable states and phase-shifts. At the same time, the concept of coral reef structural complexity has many different components and their influence is difficult to understand and quantify.

Complex dynamic systems are governed by different processes that occur simultaneously on different levels of selection (Okasha 2006). Understanding them separately as well as their interplay is one of the key goals in ecological research (Green et al. 2006). Here we used a combination of 3D geometrical metrics to paint a detailed picture of the effect of an extreme weather event on the structural dynamics of coral reefs. We found that the storm caused

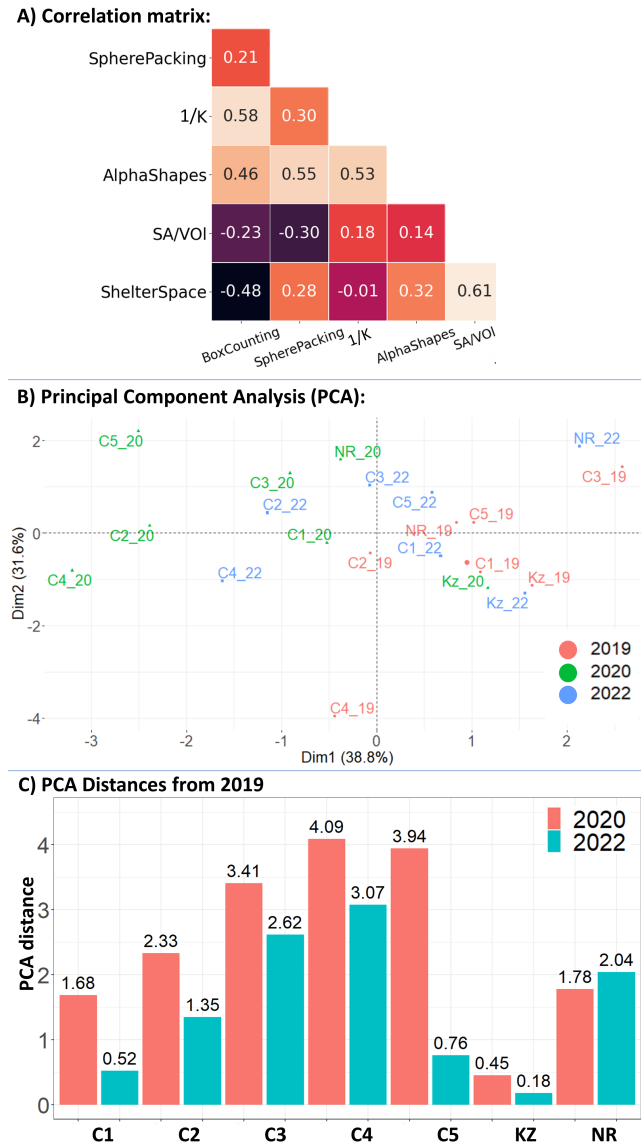

FIGURE 4 Multivariate analysis of coral reef structure over time. A) Pearson product-moment correlation coefficients of all metrics. The figure shows a low-to-moderate correlation among the variables. B) Principal component analysis (PCA) of the full data-set. Colors signify the year and reveal a clear temporal trend along PC1. C) Euclidean distance on two PC axes between years per site, with the 2019 models as reference. Color indicates year. The distances are shorter in 2019-2022 (red) than in 2019-2022 (blue).

a decrease in structural complexity, and that in two years after the disturbance the reefs regained some of their structural attributes. This suggests that the disturbance (powerful storm) did not cause a phase-shift in the reef w.r.t. to structural complexity. Therefore in the setting of this study: structure as a proxy for the phase of the system, storm

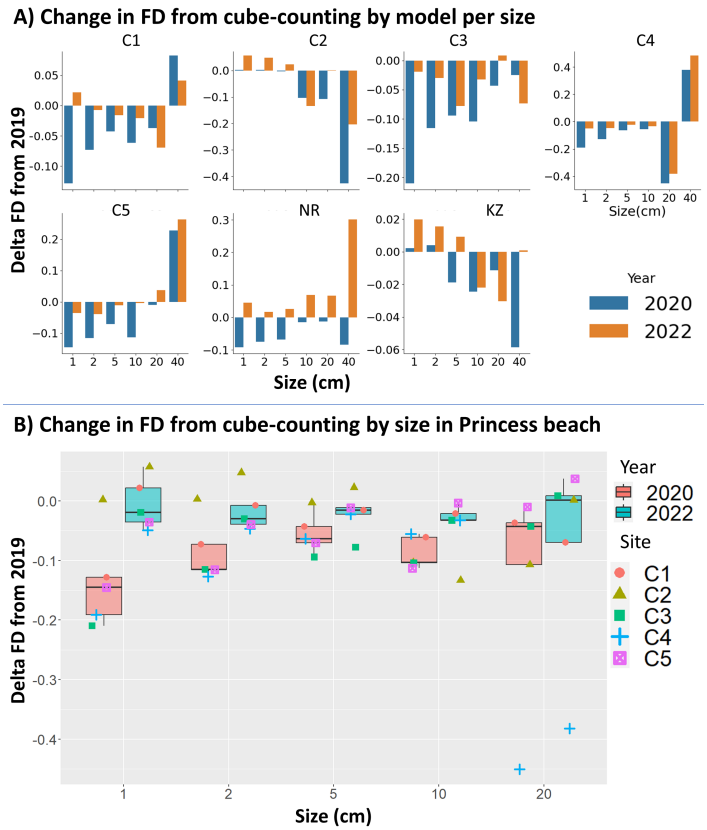

FIGURE 5 Comparison of FD by size-category using cube counting. A) The changes by size category (cube size) per site compared to 2019 as a baseline. We calculated the slope between two consecutive measurements in cube counting and attributed the value to the smaller box size (see methods 2.3.1). B) The changes in Princess beach sites (C1-C5) by size category. The sites are marked by shape and color, and the years are aggregated in the boxes. The blue boxes are higher than the red boxes showing that there was more difference (decline) in FD in 2020 than in 2022.

as the imposed disturbance, and the spatial and temporal bounds of seven reef sites over three years- the reef is resilient.

Fractal dimension in reef ecology has been measured in various ways for several decades (Bradbury et al. 1983). However, these measurements were largely confined by the available technological tools. The new era of underwater photogrammetry (Ferrari et al. 2022) unleashes the opportunity to study reefs in 3D, in accuracy and detail across large scales, leading FD to become one of the most common descriptors for coral reef ecology. We used three methods to calculate FD: cube counting, alpha-shapes/SA, and sphere-packing (Reichert et al. 2017). As opposed to previous works, our implementations for calculating FD (cube-counting and alpha-shapes/SA) leverage the full 3D model rather than a 2.5D representation (single Z value per coordinate), and perform on the entire reef scale rather than single coral colonies. This is important in light of the input: reef knolls that contain overhangs and crevices.

Cube-counting and alpha-shapes/SA are effective methods that were indicative individually of decline and recov-

ery in structural complexity (Fig. 3). The main disadvantage of cube counting is that it is an extrinsic calculation. It is sensitive to rotation and registration errors since the minimal bounding cube (the first iteration of the algorithm) is axis-aligned on an external grid. An interesting follow-up study would focus on finding a rotation-invariant minimal bounding cube. That would eliminate the need for registration in temporal comparisons. We chose to introduce a new surface based measure using alpha-shapes because it enables calculating FD without reducing the Z axis (Young et al. 2017). Alpha-shapes/SA is an intrinsic method that is not sensitive to rotation because it operates on the model directly without considering the external coordinate system (grid). A disadvantage is that sometimes the alpha filter causes distant areas of the mesh to merge together resulting in a reverse ratio (low alpha value with low surface area).

Calculating FD by size-category from cube-counting enables choosing the scales of investigation (Figs. 4, 1) (Backes and Bruno 2012). Defining the relevant contribution of each size class to an observation, i.e., structural complexity measurements, can lead to a better understanding of the overarching process. For example in our case, we attribute the decrease in FD in large size-categories to whole colony removal by the storm, and an increase in the small size-categories is attributed to coral recruitment and growth.

Shelter-space and SA/Vol are sensitive to the models footprint (the size of the models base, the area that the knoll captures on the sand/substrate), especially shelter space which uses a convex hull function (crude encapsulation of the model). For example, these metrics have extreme values for C4 2019 that are caused by a large footprint of the 3D model which was reduced after the storm. Registering the models before cropping the area of interest can help to overcome this bias.

Model registration is important for visualizing changes in the reef as well as for calculating rotation variant methods (extrinsic methods, e.g., cube-counting). However, the registration is difficult because the scenes are dynamic. External coordinates (e.g., GPS) could help to register the models over time yet they are difficult to obtain underwater. An important follow-up study would focus on defining the error of registration in practical terms, i.e., the amount of growth/decay (signal) which can be captured. This can be done by imaging the same reef several times in the same day and registering the models assuming there is no change (Yuval et al. 2021).

One of the main shortcomings of this study is the variance in the number of images collected in each survey. Ideally, we would have a consistent amount of images per surface area depicted. However, we wanted to guarantee a high-quality reconstruction of the reef. Therefore, the third survey round had a larger number of images per site and a higher-quality reconstruction which affects the complexity score (more complex). We solve this in cube counting and alpha-shapes by measuring above the size of reconstruction quality artifacts: the smallest bounding cube is one cm^3 and the smallest alpha value is 2.5 cm.

Coral reefs are some of the most intricate and diverse ecosystems on the planet, and the problem of scale vs. detail in coral reef ecological studies has yet been brought to bear. The most important follow-up study will measure coral growth and decay directly by tracking the same colonies over time (Fig.2B). Although there are tools for fast segmentation of benthic maps (Pavoni et al. 2022), there are almost no available tools for 3D segmentation and accurate size measurements in complex 3D scenes (Petrovic et al. 2014). 3D segmentation tools still require manual annotations that limit their scalability. On the contrary, using only geometry is scalable but provides limited detail, i.e., lacking taxonomic information.

We release the ***Reefs4D*** data-set, which is scarce in the computer-vision and 3D graphics community and can lead to exciting research. We expect that in the near future 3D instance-segmentation (a deep-learning task that segments every object in a model) together with geometric deep-learning will enable studies that include taxonomic information together with geometry and reef structure. Altogether, computer-vision with advances in scalable conservation technologies such as sound recordings (Williams et al. 2022) and metagenomics (Levy et al. 2023) will enable a new generation of multi-modal studies in coral reef ecology.

Corals dominate many shallow marine habitats and powerful storms are inseparable from their evolution. Nevertheless, such acute disturbances can cause coral reefs to become more vulnerable to local disturbances (e.g., pollution, tourism), which in turn can lead to an ecosystem collapse. In light of the increasing frequency of disturbances, it is important to continue tracking reefs over large areas and long periods of time. Our work provides an important baseline and methodology for such efforts.

Declarations

- Funding: T.T. was supported by the Leona M. and Harry B. Helmsley Charitable Trust, the Maurice Hatter Foundation, the Israel Ministry of National Infrastructures, Energy and Water Resources Grant 218-17-008, the Israel Ministry of Science, Technology and Space grant 3-12487, and the Technion Ollendorff Minerva Center for Vision and Image Sciences. M.Y. was supported by the Data Science Research Center at the University of Haifa, the Murray Foundation for student research, and Microsoft AI for Earth; AI for Coral Reef Mapping. This research was supported by the Israel Data Science Initiative (IDSI) of the Council for Higher Education in Israel and the Data Science Research Center at the University of Haifa.
- Author Contributions: **All authors:** Conceptualization, Writing—Review and Editing. **M.Y., N.P:** Software, Methodology, Visualization. **M.Y.:** Formal analysis, Investigation, Data Curation, Writing—Original Draft. **T.T:** Supervision.

Acknowledgments

We thank the Interuniversity Institute for Marine Sciences of Eilat for making their facilities available to us. We thank Aviad Avni and Opher Bar-Nathan for valuable intellectual and technical contributions; Netta Kasher for drawing Fig. 2A; Fieldwork in Eilat was carried out under permit 42-128 from the Israeli Nature and Parks Authority. The authors declare no conflict of interest.

conflict of interest

The authors declare no conflict of interest

references

Alvarez-Filip, L., Dulvy, N. K., Gill, J. A., Côté, I. M. and Watkinson, A. R. (2009) Flattening of caribbean coral reefs: region-wide declines in architectural complexity. *Proceedings of the Royal Society B: Biological Sciences*, **276**, 3019–3025.

Aston, E. A., Duce, S., Hoey, A. S. and Ferrari, R. (2022) A protocol for extracting structural metrics from 3d reconstructions of corals. *Frontiers in Marine Science*, **9**, 854395.

Backes, A. R. and Bruno, O. M. (2012) Fractal and multi-scale fractal dimension analysis: a comparative study of bouligand-minkowski method. *arXiv preprint arXiv:1201.3153*.

Barnsley, M. F. (2014) Fractals everywhere.

Bradbury, R. R., Reichelt, R. R. et al. (1983) Fractal dimension of a coral reef at ecological scales. *Marine Ecology Progress Series-pages: 10: 169-171*.

Cignoni, P., Callieri, M., Corsini, M., Dellepiane, M., Ganovelli, F. and Ranzuglia, G. (2008) MeshLab: an Open-Source Mesh Processing Tool.

CloudCompare, G. (2022) Cloudcompare. URL: http://www.cloudcompare.org/.

Connell, J. H. and Sousa, W. P. (1983) On the evidence needed to judge ecological stability or persistence. *The American Naturalist*, **121**, 789–824.

Crisp, S. K., Tebbett, S. B. and Bellwood, D. R. (2022) A critical evaluation of benthic phase shift studies on coral reefs. *Marine Environmental Research*, 105667.

Dudgeon, S. R., Aronson, R. B., Bruno, J. F. and Precht, W. F. (2010) Phase shifts and stable states on coral reefs. *Marine Ecology Progress Series*, **413**, 201–216.

Edelsbrunner, H., Kirkpatrick, D. and Seidel, R. (1983) On the shape of a set of points in the plane. *IEEE Transactions on information theory*, **29**, 551–559.

Ferrari, R., Bryson, M., Bridge, T., Hustache, J., Williams, S. B., Byrne, M. and Figueira, W. (2016) Quantifying the response of structural complexity and community composition to environmental change in marine communities. *Global change biology*, **22**, 1965–1975.

Ferrari, R., Gonzalez-Rivero, M., Leon, J. X., Burns, J. H., Figueira, W. F., Sandin, S. A. and Davies, A. J. (2022) Advances in 3d habitat mapping of marine ecosystem ecology and conservation.

Friedman, A., Pizarro, O., Williams, S. B. and Johnson-Roberson, M. (2012) Multi-scale measures of rugosity, slope and aspect from benthic stereo image reconstructions. *PloS one*, **7**, e50440.

Fukunaga, A. and Burns, J. H. (2020) Metrics of coral reef structural complexity extracted from 3d mesh models and digital elevation models. *Remote Sensing*, **12**, 2676.

George, E. E., Mullinix, J. A., Meng, F., Bailey, B. A., Edwards, C., Felts, B., Haas, A. F., Hartmann, A. C., Mueller, B., Roach, T. N. et al. (2021) Space-filling and benthic competition on coral reefs. *PeerJ*, **9**, e11213.

Graham, N. A. and Nash, K. L. (2013) The importance of structural complexity in coral reef ecosystems. *Coral reefs*, **32**, 315–326.

Green, D. G., Klomp, N., Rimmington, G. and Sadedin, S. (2006) Complexity in landscape ecology.

Gunderson, L. H. (2000) Ecological resilience–in theory and application. *Annual review of ecology and systematics*, 425–439.

Halley, J., Hartley, S., Kallimanis, A., Kunin, W., Lennon, J. and Sgardelis, S. (2004) Uses and abuses of fractal methodology in ecology. *Ecology letters*, **7**, 254–271.

Harmelin-Vivien, M. L. (1994) The effects of storms and cyclones on coral reefs: a review. *Journal of Coastal Research*, 211–231.

Hoegh-Guldberg, O. and Bruno, J. F. (2010) The impact of climate change on the world's marine ecosystems. *Science*, **328**, 1523–1528.

Holling, C. S. (1973) Resilience and stability of ecological systems. *Annual review of ecology and systematics*, 1–23.

Hughes, T. P. (1994) Catastrophes, phase shifts, and large-scale degradation of a caribbean coral reef. *Science*, **265**, 1547–1551.

Hughes, T. P., Baird, A. H., Bellwood, D. R., Card, M., Connolly, S. R., Folke, C., Grosberg, R., Hoegh-Guldberg, O., Jackson, J. B., Kleypas, J. et al. (2003) Climate change, human impacts, and the resilience of coral reefs. *science*, **301**, 929–933.

Hughes, T. P., Barnes, M. L., Bellwood, D. R., Cinner, J. E., Cumming, G. S., Jackson, J. B., Kleypas, J., Van De Leemput, I. A., Lough, J. M., Morrison, T. H. et al. (2017) Coral reefs in the anthropocene. *Nature*, **546**, 82–90.

Hylkema, A., Debrot, A. O., Osinga, R., Bron, P. S., Heesink, D. B., Izioka, A. K., Reid, C. B., Rippen, J. C., Treibitz, T., Yuval, M. et al. (2020) Fish assemblages of three common artificial reef designs during early colonization. *Ecological Engineering*, **157**, 105994.

Jackson, J. B. and Hughes, T. P. (1985) Adaptive strategies of coral-reef invertebrates: coral-reef environments that are regularly disturbed by storms and by predation often favor the very organisms most susceptible to damage by these processes. *American Scientist*, **73**, 265–274.

Jones, C. G., Lawton, J. H. and Shachak, M. (1994) Organisms as ecosystem engineers. *Ecosystem management*, 130–147.

Knudby, A. and LeDrew, E. (2007) Measuring structural complexity on coral reefs. *Proceedings of the American Academy of Underwater Sciences 26th Symposium*, 181–188.

Levy, N., Simon-Blecher, N., Ben-Ezra, S., Yuval, M., Doniger, T., Leray, M., Karako-Lampert, S., Tarazi, E. and Levy, O. (2023) Evaluating biodiversity for coral reef reformation and monitoring on complex 3d structures using environmental dna (edna) metabarcoding. *Science of The Total Environment*, **856**, 159051.

Mandelbrot, B. (1967) How long is the coast of britain? statistical self-similarity and fractional dimension. *science*, **156**, 636–638.

McCarthy, O. S., Smith, J. E., Petrovic, V. and Sandin, S. A. (2022) Identifying the drivers of structural complexity on hawaiian coral reefs. *Marine Ecology Progress Series*, **702**, 71–86.

Nash, K. L., Graham, N. A., Wilson, S. K. and Bellwood, D. R. (2013) Cross-scale habitat structure drives fish body size distributions on coral reefs. *Ecosystems*, **16**, 478–490.

Nyström, M. and Folke, C. (2001) Spatial resilience of coral reefs. *Ecosystems*, **4**, 406–417.

Okasha, S. (2006) *Evolution and the levels of selection*. Clarendon Press.

Pascoe, K. H., Fukunaga, A., Kosaki, R. K. and Burns, J. H. (2021) 3d assessment of a coral reef at lalo atoll reveals varying responses of habitat metrics following a catastrophic hurricane. *Scientific reports*, **11**, 1–9.

Pavoni, G., Corsini, M., Ponchio, F., Muntoni, A., Edwards, C., Pedersen, N., Sandin, S. and Cignoni, P. (2022) Taglab: Ai-assisted annotation for the fast and accurate semantic segmentation of coral reef orthoimages. *Journal of field robotics*, **39**, 246–262.

Petrovic, V., Vanoni, D. J., Richter, A. M., Levy, T. E. and Kuester, F. (2014) Visualizing high resolution three-dimensional and two-dimensional data of cultural heritage sites. *Mediterranean Archaeology and Archaeometry*, **14**, 93–100.

Porter, J. W., Woodley, J. D., Smith, G. J., Neigel, J. E., Battey, J. F. and Dallmeyer, D. G. (1981) Population trends among jamaican reef corals. *Nature*, **294**, 249–250.

Reichert, J., Backes, A. R., Schubert, P. and Wilke, T. (2017) The power of 3d fractal dimensions for comparative shape and structural complexity analyses of irregularly shaped organisms. *Methods in Ecology and Evolution*, **8**, 1650–1658.

Roff, G. and Mumby, P. J. (2012) Global disparity in the resilience of coral reefs. *Trends in ecology & evolution*, **27**, 404–413.

Rogers, A., Blanchard, J. L. and Mumby, P. J. (2014) Vulnerability of coral reef fisheries to a loss of structural complexity. *Current Biology*, **24**, 1000–1005.

Rogers, C. S. (1993) Hurricanes and coral reefs: the intermediate disturbance hypothesis revisited. *Coral Reefs*, **12**, 127–137.

Standish, R. J., Hobbs, R. J., Mayfield, M. M., Bestelmeyer, B. T., Suding, K. N., Battaglia, L. L., Eviner, V., Hawkes, C. V., Temperton, V. M., Cramer, V. A. et al. (2014) Resilience in ecology: Abstraction, distraction, or where the action is? *Biological Conservation*, **177**, 43–51.

Sugihara, G. and May, R. M. (1990) Applications of fractals in ecology. *Trends in Ecology & Evolution*, **5**, 79–86.

Torres-Pulliza, D., Dornelas, M. A., Pizarro, O., Bewley, M., Blowes, S. A., Boutros, N., Brambilla, V., Chase, T. J., Frank, G., Friedman, A. et al. (2020) A geometric basis for surface habitat complexity and biodiversity. *Nature Ecology & Evolution*, **4**, 1495–1501.

Urbina-Barreto, I., Chiroleu, F., Pinel, R., Fréchon, L., Mahamadaly, V., Elise, S., Kulbicki, M., Quod, J.-P., Dutrieux, E., Garnier, R. et al. (2021) Quantifying the shelter capacity of coral reefs using photogrammetric 3d modeling: From colonies to reefscapes. *Ecological Indicators*, **121**, 107151.

Walsh, J. and Watterson, J. (1993) Fractal analysis of fracture patterns using the standard box-counting technique: valid and invalid methodologies. *Journal of structural Geology*, **15**, 1509–1512.

Williams, B., Lamont, T. A., Chapuis, L., Harding, H. R., May, E. B., Prasetya, M. E., Seraphim, M. J., Jompa, J., Smith, D. J., Janetski, N. et al. (2022) Enhancing automated analysis of marine soundscapes using ecoacoustic indices and machine learning. *Ecological Indicators*, **140**, 108986.

Young, G., Dey, S., Rogers, A. and Exton, D. (2017) Cost and time-effective method for multi-scale measures of rugosity, fractal dimension, and vector dispersion from coral reef 3d models. *PloS one*, **12**, e0175341.

Yuval, M., Alonso, I., Eyal, G., Tchernov, D., Loya, Y., Murillo, A. C. and Treibitz, T. (2021) Repeatable semantic reef-mapping through photogrammetry and label-augmentation. *Remote Sensing*, **13**, 659.

Supporting Information

The results of structural complexity calculations, the number of images, and location of the models.

Model	Year	BoxCounting	SpherePacking	1/K	Alpha/SA	SA/VOl	SA	Vol	ChullVol	Shelter	#Images	Lat	Lon
C1	2019	2.190	1.669	0.799	2.295	10.848	32.663	3.011	7.151	0.579	226	29.49358	34.90619
C1	2020	2.177	1.599	0.708	2.264	10.121	22.984	2.271	4.985	0.544	265	29.49358	34.90619
C1	2022	2.207	1.576	0.775	2.291	11.724	23.038	1.965	4.349	0.548	494	29.49358	34.90619
C2	2019	2.198	1.541	0.763	2.262	11.990	18.921	1.578	3.491	0.548	200	29.49364	34.90618
C2	2020	2.149	1.458	0.693	2.199	10.581	12.443	1.176	2.436	0.517	226	29.49364	34.90618
C2	2022	2.210	1.450	0.728	2.220	11.271	12.545	1.113	2.290	0.514	352	29.49364	34.90618
C3	2019	2.263	1.726	0.876	2.283	9.152	45.358	4.956	8.710	0.431	448	29.4943	34.90678
C3	2020	2.177	1.611	0.712	2.230	7.659	22.486	2.936	5.345	0.451	159	29.4943	34.90678
C3	2022	2.207	1.596	0.743	2.252	8.872	23.289	2.625	4.920	0.467	409	29.4943	34.90678
C4	2019	2.154	1.488	0.805	2.265	21.799	19.499	0.894	2.755	0.675	305	29.49411	34.90677
C4	2020	2.106	1.532	0.595	2.215	11.023	18.077	1.640	3.765	0.564	196	29.49411	34.90677
C4	2022	2.146	1.462	0.690	2.258	12.922	20.313	1.572	3.553	0.558	462	29.49411	34.90677
C5	2019	2.205	1.511	0.823	2.307	11.470	16.540	1.442	2.678	0.462	241	29.49462	34.90703
C5	2020	2.174	1.475	0.635	2.203	8.109	11.774	1.452	2.288	0.365	204	29.49462	34.90703
C5	2022	2.238	1.481	0.755	2.299	11.361	14.394	1.267	2.241	0.435	308	29.49462	34.90703
Kazaa	2019	2.186	1.849	0.737	2.327	10.318	89.324	8.657	21.188	0.591	832	34.93437	34.93437
Kazaa	2020	2.181	1.840	0.747	2.293	9.599	78.811	8.210	22.276	0.631	648	34.93437	34.93437
Kazaa	2022	2.189	1.826	0.754	2.316	10.828	82.933	7.659	19.602	0.609	767	34.93437	34.93437
NR	2019	2.201	1.570	0.776	2.307	9.246	32.018	3.463	7.051	0.509	392	29.50941	34.92394
NR	2020	2.184	1.633	0.802	2.203	8.327	27.164	3.262	5.610	0.419	495	29.50941	34.92394
NR	2022	2.318	1.641	0.763	2.299	10.095	30.690	3.040	5.204	0.416	629	29.50941	34.92394
Median	NA	2.189	1.576	0.754	2.265	10.581	22.984	2.271	4.920	0.517	352	29.4943	34.90678
Std	NA	0.044	0.126	0.063	0.041	2.860	23.417	2.363	6.236	0.081	195	1.9498	0.01083

TABLE 1 summary of the metrics for structural complexity assessment